Published in final edited form as:
Nat Synth. 2023 January ; 2(1): 26–36. doi:10.1038/s44160-022-00191-5.

Unveiling the impact of the light-source and steric factors on [2+2] heterocycloaddition reactions

Javier Mateos[1], **Francesco Rigodanza**[1], **Paolo Costa**[1], **Mirco Natali**[2], **Alberto Vega-Peñaloza**[1], **Elisa Fresch**[1], **Elisabetta Collini**[1], **Marcella Bonchio**[1], **Andrea Sartorel**[1], **Luca Dell'Amico**[1,*]

[1]Department of Chemical Sciences, University of Padova, Via Marzolo 1, 35131 Padova, Italy

[2]Dipartimento di Scienze Chimiche e Farmaceutiche, University of Ferrara, Via Luigi Borsari 46, 44121 Ferrara, Italy

Abstract

Information gained from in-depth mechanistic investigations can be used to control the selectivity of reactions, leading to the expansion of the generality of synthetic processes and the discovery of new reactivity. Here, we investigate the mechanism of light-driven [2+2] heterocycloadditions (Paternò-Büchi reactions) between indoles and ketones to develop insight into these processes. Using ground-state UV-Vis absorption and transient absorption spectroscopy (TAS), together with DFT calculations, we found that the reactions can proceed via an exciplex or electron-donor-acceptor (EDA) complex, which are key intermediates in determining the stereoselectivity of the reactions. We used this discovery to control the diastereoselectivity of the reactions, gaining access to previously inaccessible diastereoisomeric variants. When moving from 370 to 456 nm irradiation, the EDA complex is increasingly favoured, and the diastereomeric ratio (d.r.) of the product moves from >99:<1 to 47:53. In contrast, switching from methyl to ^{i}propyl substitution favours the exciplex intermediate, reversing the d.r. from 89:11 to 16:84. Our study shows how light and steric parameters can be rationally used to control the diastereoselectivity of photoreactions, creating mechanistic pathways to previously inaccessible stereochemical variants.

Abstract

Correspondence and requests for materials should be addressed to Luca Dell'Amico.

Author contributions

J. M. and L.D. wrote the manuscript with contributions from all the authors. J. M. and L. D. conceived the project and devised the experiments. J. M. and A. V. carried out the reactions and isolated and characterized the products. J. M., L. D., M. B. and A. S. rationalized the experimental results. F. R., M. N, E. C. and E. F. performed the spectroscopic investigations using TAS. P.C. and A. S. performed the DFT calculations.

Competing interests

All the authors declare no competing interests.

Europe PMC Funders Author Manuscripts

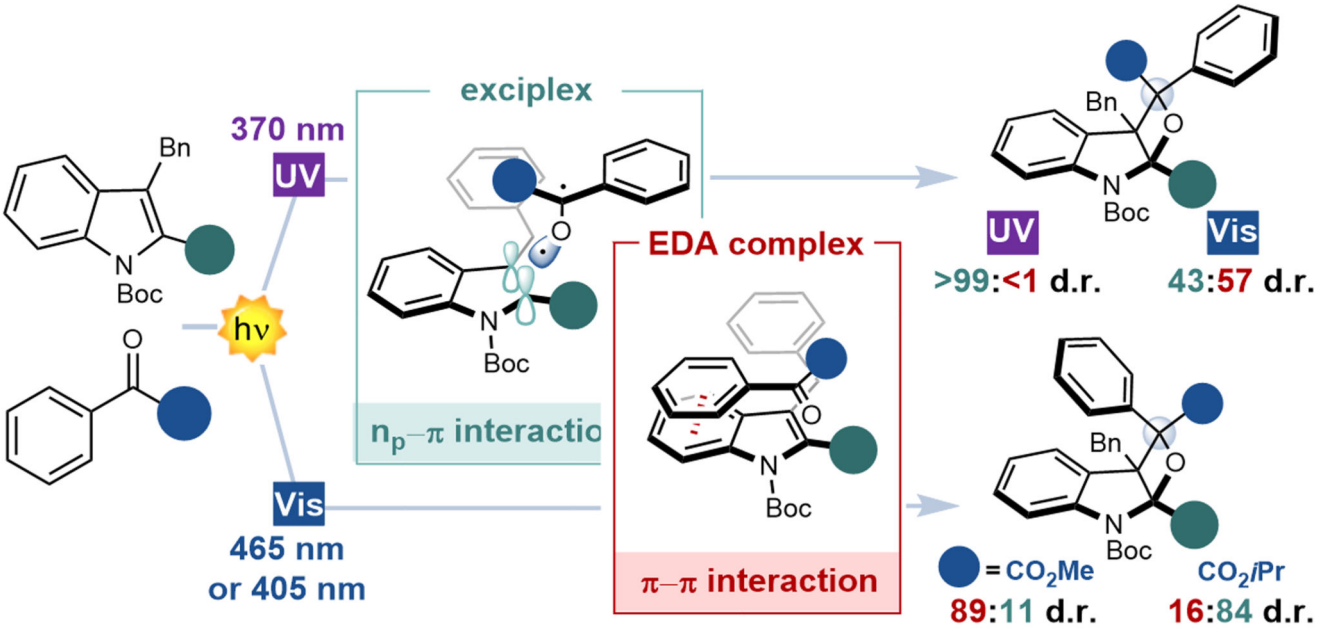

Introduction

Synthetic photochemistry has grown tremendously in the past decade[1] and radical species are no longer considered to be difficult-to-handle intermediates[2]. Selective visible-light synthetic methods have been rapidly developed alongside photoredox catalysis[3] and milder visible-light sources have been used for popular light-driven reactions that were historically performed under UV-light irradiation[4–6]. The long-studied Paternò-Büchi (PB) reaction is a light-driven [2+2] heterocycloaddition reaction between an olefin and a carbonyl compound[7, 8]. As first described by Paternò in 1909, this formidable light-driven reaction leads, in a single step, to a strained oxetane, which is often present in natural products and drugs[9]. This reaction and other light-driven processes have been the subject of intense mechanistic investigations (Fig. 1a), which identified diverse and divergent reaction manifolds[10–13]. In 1954, Büchi reported that, in PB reactions, the ground-state olefin reacts with the triplet excited state (T_1) of the carbonyl counterpart, generating a 1,4 biradical intermediate (Fig. 1a, left)[8, 14, 15]. In 1972, Turro reported the possibility of generating an exciplex between the reagents, possibly leading to different product distributions.[10, 12] A few years later, Mattay reported that, when a charge-transfer (CT) complex between the reagents forms, the reaction proceeds through a more selective concerted mechanism[11].

The formation of a CT state proceeds through either an exciplex between an electron-rich olefin and the excited ketone, or the formation of an electron-donor-acceptor (EDA) complex, which is a ground-state association characterized by a red-shifted absorption with respect to the single reactants[16]. Importantly, the spatial arrangement of the reagents determines the geometries of the CT states and the final oxetane stereochemistry[17]. As hypothesized by Kochi[18], different stereoisomers can emerge when the cycloaddition process passes through different CT states, which lead to different spatial arrangements (for

Europe PMC Funders Author Manuscripts

example, exciplex versus EDA complex) (Fig. 1b). In these cases, the wavelength selection is relevant for the stereochemical outcome. This hypothesis is confirmed by light-driven processes which use new types of substrates that can generate EDA complexes (such as indoles)[19, 20]. These scaffolds allow broad control over the electronic and steric parameters. By using different indole-derived heterocycles, it is thus possible to channel the reactivity towards the intended stereochemical variant[21].

Based on detailed mechanistic investigations, we herein report how to control the stereochemical outcome of light-driven [2+2] heterocycloadditions. Our study includes biorelevant indole heterocycles, aromatic ketones, and α-ketoesters. We rationalized our experimental findings by using various spectroscopic techniques, ground state and transition absorption spectroscopy (TAS), emission spectroscopy, and DFT calculations (Fig. 1c). By manipulating specific physicochemical parameters (light source or steric factors), the reaction's diastereoselectivity can be deliberately altered towards the activity of two stereodivergent reaction manifolds (exciplex versus EDA complex), leading to opposite diastereomers. These findings were extended to different indole derivatives and implemented under continuous flow irradiation, allowing access to elusive stereochemical variants on a preparative scale.

Results and discussion

Spectroscopic identification of three different reaction manifolds

We initiated our study by selecting as the mechanistic probe the [2+2] heterocycloaddition reaction between indoles **1a**-**b** and aryl ketones **2a**-**b** (Fig. 2), where no diastereoselection is envisaged due to the symmetric nature of the ketone (see Supplementary Section E). Interestingly, we discovered that according to our experimental findings, and in agreement with literature, the reaction can proceed through three alternative reaction manifolds (pathways i-iii in Fig. 2), leading to a single regio- and diastereoisomer.

Conventional triplet mechanism – pathway i

When indole **1a** and benzophenone **2a** are involved (Fig. 2, top), a conventional radical trapping mechanism is observed[18, 19]. This is a PB process commonly mediated by a UV-light source (250-360 nm) that promotes, after intersystem crossing (ISC) from the singlet state, the generation of the long-lived triplet state (T_1). The T_1 is then trapped by the electron-rich **1a** (triplet-state **I** in Fig. 2, top), generating the corresponding 1,4-biradical **4**. This mechanism was confirmed by TAS-experiments at a ns scale (Fig. 2, top-right 1,4-biradical box). In fact, by TAS, we observed the decay of the T_1 (max abs. at 525 nm) along with the concomitant appearance of the 1,4-biradical **4** (max abs. at 390 nm)[22]. This transient intermediate leads to the oxetane product **3a** within a hundred ns (see Supplementary Section C). The experimental data clearly suggest a pure-triplet mechanism as the only operative pathway, as no traces of a radical ion-pair (IP) were detected. Additionally, a PET (photoinduced electron transfer) pathway can be excluded owing to its high endergonicity (ΔG_{PET} = 10.3 kcal·mol^{-1}). Importantly, it is well documented by several literature reports that when the $\Delta G_{PET} > 0$ kcal·mol^{-1}, PET processes are prevented and the reaction proceeds through a radical-trapping mechanism[23, 24].

Exciplex-based pathway - pathway ii

In the presence of a more electron-deficient ketone such as **2b** (*m*-CF_3 benzophenone) and under diluted conditions ([**2b**] = 0.01M in acetone) (Fig. 2, middle) we observed an alternative mechanism. Analogously to pathway i, no ground state interactions between **1a** and **2b** were detected (see Supplementary Section C). Nevertheless, TAS experiments revealed the appearance of the transient radical IP (**5** + **6**) upon T_1 decay, as supported by the spectral changes at λ=780 nm characteristic of the benzophenone radical anion (Fig. 2, radical-ion-pair box and Supplementary Sections C and D). Additionally, no traces of the biradical **4** were observed at λ < 400 nm, indicating that the radical IP evolves through a concerted or quasi-concerted mechanism to the oxetane product **3**[25]. This data implies that after the ketone excitation, the T_1 state of **2b** interacts with the indole generating the exciplex **II**, that possesses a charge transfer character consistent with the exergonicity of the photoinduced electron transfer (PET) process (ΔG_{PET} = - 9.7 kcal·mol^{-1}). The direct spectroscopic signature of the exciplex was investigated for benzil **7** and indole **1b** (vide infra). This is because the low visible-light absorption of benzophenone **2b** at 405 nm led to the selective excitation of the EDA complex with a negligible contribution of the ketone direct excitation.

EDA-complex-based pathway - pathway iii

This pathway foresees the interaction of the two reactants at the ground state level into an EDA complex under more concentrated conditions ([**2b**] = 0.1 M in Acetone) (Fig. 2, bottom). UV-Vis titration experiments with the electron-rich indole **1b** and the electron-poor benzophenone **2b**, revealed the appearance of a red-shifted CT band (Fig. 2, EDA complex, bottom left). A modest binding constant (K_{EDA} = 0.47 M^{-1}, in acetone at 25 °C) was extrapolated for the equilibrium of formation of the complex (see Supplementary Section C). Within an EDA-complex-based manifold, a stereochemically alternative radical IP (**5** + **6**) is directly produced upon PET (λ_{max} 723 nm). As monitored by TAS, a favourable PET process (ΔG_{PET} = -9.7 kcal·mol^{-1}) occurs delivering the radical IP, whose spectral assignment is confirmed by spectroelectrochemistry (Fig. 2, alternative radical-ion-pair box and Supplementary Sections C and D). This species decays with a time-constant of 180 ns into the oxetane product.

We envisaged that the three diverse reaction manifolds observed by TAS are governed by alternative orbital interactions. For instance, the interactions within pathway iii differ from pathway i and pathway ii, which lack the **π** orbital overlap of the indole with the half-filled n_P orbital of the excited ketone. Indeed, it is well established that for EDA-complexes alternative **π**–**π** interactions are relevant[16]. Importantly, diverse orbital interactions may lead to diverse spatial orientations of the reagents and finally alter the stereoselectivity of the process. For this reason, we decided to gain insights into the diverse molecular orientations by using DFT methods.

Computational insights into the exciplex versus the EDA-complex pathway

Aiming at developing a novel stereodivergent process, we focused our attention on the exciplex-based pathway ii and the EDA-complex-based pathway iii, with **1b** and **2b** as reactants.

Under diluted conditions ([**2b**] = 0.01 M in acetone), no EDA complex is detected, meaning that under these conditions the only active pathway is the exciplex-based pathway ii. Conversely, when more concentrated conditions ([**2b**] = 0.1 M in acetone) are used the EDA-complex pathway iii starts to be competitive.

To gain insight into the two diverse arrangements involved in the PET-based pathways (exciplex versus EDA complex), we employed DFT calculations at the (U)M06-2X/6-311++G(d,p)/_IEFPCM(acetone) level of theory (Fig. 3)[17]. This functional is a well-established method to describe charge transfer complexes both in singlet and triplet states[26,27].

Excited-state (T_1) exciplex arrangement, pathway ii

Upon direct excitation of the ketone **2b**, the corresponding T_1 state is generated (Fig. 3a). At this juncture, the T_1 interacts with the ground state **1b**[10]. In this case, the oxygen atom of the T_1 **2b** and the C2 position of **1b** are in close proximity (Fig. 3a, n_p-π interaction, 2.56 Å). Interestingly, the spin density map of the computed exciplex is almost equally distributed between the indole and the ketone (1.03 and 0.97 respectively (Fig. 3)). However, a large dipole moment is observed upon excitation (μ=15.6 D). This altered charge distribution indicates a remarkable CT character as reflected by natural population analysis. In fact, a total of 0.90 charge unit is transferred from indole to the ketone, corroborating the PET-based pathway ii, where the radical ion-pair has been detected experimentally by laser flash photolysis (LFP) measurements.

Ground-state (S0) EDA-complex arrangement, pathway iii

As experimentally observed, when concentrated conditions are used ([**2b**]=0.1 M in acetone) an EDA-complex is generated between the reagents (Fig. 3b). This complex is held together through a π–π stacking interaction between the electron-rich aromatic ring of indole **1b** and the electron-poor aromatic ring of the ketone **2b** (interaction ~3.6 Å (Fig. 3) and corroborated by computed UV-Vis spectra in Supplementary Fig. S.I.8.)[27, 28]. Additionally, the analysis of the frontier molecular orbitals of the EDA-complex reveals that the HOMO is located on the indole moiety while the LUMO is distributed along the ketone resulting in a dipole moment (μ) of 4.8 D (Fig. 3). To better elucidate the photoinduced electron transfer observed after irradiation of the EDA complex, we performed vertical excitation calculations employing a time-dependent density functional theory (TD-DFT) method. This technique allowed us to analyze the corresponding excited state involved in the PET process. For the S_1 excited-state, a HO-MO-LUMO contribution of 83.5% has been computed (3.66 eV), showing a remarkable charge transfer character (Fig. 3, μ=16.2 D). Indeed, natural population analysis of S_1 indicates that upon vertical excitation of the EDA complex a substantial charge (0.79) is transferred from the indole moiety **1b** to the ketone **2b**, which resembles the experimentally observed radical ion-pair system.

The impact of the light source on the diastereodifferenciation process

Based on the different geometries and orbital interactions obtained by DFT calculations (Fig. 4), it is possible to represent the two alternative reaction manifolds by using a simplified potential energy surface diagram (Fig. 4b)[28]. The spatial arrangements of the molecules are retained and directly transferred to the final oxetane product due to the concerted-character of PET-based PB reactions[11, 12]. For instance, when the reaction mixture is irradiated at 405 nm, the CT-band of the EDA complex is directly excited (Fig. 4b left, red lines). This irradiation leads to the formation of a radical IP with a preferred **π–π** interaction. However, **2b** can be directly excited at 370 nm. In this case the n_p-**π** interaction will govern the spatial arrangement of the IP (Fig. 4b right, green lines). Thus, a light stereodifferentiation process can occur when switching the irradiation source from UV- to visible-light.

As per the DFT calculations, there are two alternative sets of interactions, which do not result in any product diversification when using symmetric benzophenones. These are crucial when moving to prochiral carbonyls. We therefore evaluated benzil **7**, which is a class of synthetically relevant prochiral carbonyls used in several polar and radical reactions (Fig. 4a)[29, 30]. We hypothesized that the *endo:exo* selectivity[24] of the reaction would depend on the competition between the two alternative reaction manifolds (exciplex versus EDA complex). The conventional pure-triplet mechanism (pathway i) was ruled out by the LFP experiments of **7** with **1b** (see Supplementary Section F), which instead confirmed the photogeneration of the CT state, in agreement with the favorable ΔG_{PET} (-5.8 kcal·mol^{-1}). Thus, by altering the irradiation wavelength and the parameters that influence the EDA complex formation, the *endo:exo* selectivity can be deliberately altered in a diastereodivergent light-driven process (see Supplementary Sections E and F). Specifically, ***8-endo*** will be the preferred product in an exciplex-based mechanism, while ***8-exo*** will be favoured following an EDA complex pathway (Fig. 4a, left). Remarkably, we observed the formation of **8-*endo*** as a single diastereoisomer when running the reaction at 370 nm (>99:<1 d.r., 370 nm Fig. 4c). The *endo* selectivity results from the direct excitation of the free ketone **7**, participating in an exciplex with **1b**.[19] As hypothesized, when moving to less energetic 405 and 456 nm irradiation wavelengths, the *exo* selectivity increases, with the d.r. moving to 77:23 (456 nm Fig. 4c, left column). This is in line with the activity of the excited EDA complex between benzil **7** and the indole **1b**, whose presence was confirmed by the UV-Vis absorption spectra (see Supplementary Sections E). Increasing the concentration from 0.01 to 0.1 M favors the EDA complex pathway, resulting in a d.r. of 93:7 and 68:32 upon irradiation at 370 and 405 nm, respectively. No significant variation was observed at 456 nm, indicating that 64:36 d.r. is the limit value under these reaction conditions (Fig. 4c). Following previous experimental observations, we reasoned that performing the reaction under reduced temperature should inhibit the interconversion between the two reaction manifolds, thus magnifying the observed light stereodifferentiation process.[31] Indeed, when running the reaction at -78 °C (in acetone-d_6 at 0.1 M), the d.r. moved from >99:<1 at 370 nm to 52:48 at 456 nm. This d.r. variation is the highest ever registered for PB light-diastereodifferentiation processes, and it confirmed our initial working hyphothesis[32–34]. Furthermore, these experimental data reveal that the choice of the light is crucial. Reproducibility issues in diastereoselective PB

processes involving heterocyclic systems can be now rationalized and possibly solved by selecting the appropriate irradiation wavelength[34]. As a control experiment, we performed a reaction in an aromatic solvent, which interferes with the π–π interactions in the EDA complex. Accordingly, when using C_6D_6 as solvent, we observed reduced activity of the EDA-complex pathway, resulting in a d.r. no lower than 80:20 at 465 nm (Fig. 4c, right column). It is worth noting that across all the performed reactions we have always observed complete regiocontrol. The change of the solvent (for example, acetone versus PhMe Reichardt parameter: acetone (electron-transition energy, ET(30) = 42.2 kcal·mol^{-1}), toluene (ET(30) = 33.9 kcal·mol^{-1}), that has been reported to have high impact on the regiocontrol of other PB processes[35, 36], did not impact the high regiocontrol of the reaction between indole **1b** and ketone **7**. This behaviour is ascribable to the high steric hindrance of the indole precursors (bearing bulky *t*Butoxy carbonyl, Boc and a *t*Bu Silyl, OTBS groups at position 2).

In addition to the experimental data, we used DFT and TD-DFT calculations to compute the two different geometries for the EDA complex between ketone **7** and indole **1b** (see Supplementary Section K). Notably, the excited state (S_2, HOMO-LUMO contribution=98.4%) of this complex in the *exo* configuration has a larger dipole moment (μ=18.6 D) than in the *endo* geometry (μ=15.4 D). This indicates a substantial charge-transfer character and is in accordance with the experimental trend.

Spectroscopical characterization of the exciplex intermediate, pathway ii

In order to confirm the key reactivity of an exciplex between substrates **1b** and **7**, we performed transient absorption spectrometry (TAS) measurements at a fs timescale (Fig. 4d-g). These experiments allowed us to investigate the dynamics of the systems within the first nanosecond after photoexcitation with a time resolution of about 150 fs (see Supplementary Section F). We compared the photophysics of the single benzil **7** in the absence and in the presence of indole **1b** (Fig. 4d and e, respectively). All the experiments were conducted under the reaction conditions ([**1b**] = [**7**] = 0.1M in acetone).

For **7**, the excitation at 400 nm results in the formation of positive excited state absorption features (ESA). At early time periods, we recorded a broad absorption band centered at about 560 nm, which gradually evolved into a sharper feature with a maximum at about 525 nm. While the literature contains few reports of the ultrafast dynamics of **7**, which are typically performed at longer time resolution, it is reasonable to assign the early time signal at 560 nm to the ESA from the instantaneously photoexcited S_1 state ($S_1 \rightarrow S_n$ transition)[37,38]. This signal quickly decays (0.3 ps) while the band at 525 nm rises with the same time constant. Once formed, this band decays over a longer timeframe than the explored 600 ps. This behaviour is in agreement with a fast $S_1 \rightarrow T_1$ ISC that moves the population from S_1 to T_1 on a sub-ps timescale, followed by the long-lived $T_1 \rightarrow T_n$ absorption at 525 nm[39].

The TAS spectra of the mixture **7**-**1b** (Fig. 4e) are qualitatively similar to the TAS spectra of **7**. This is not surprising, given that the excitation at 400 nm preferentially excites **7** and therefore its spectral features are expected to prevail in the mixture response. However, the

dynamic behaviour is significantly different, with the ESA band at 525 nm decaying much quicker in the mixture than in **7** (Fig. 4f-g). The time trace of **7** alone could be fitted with a bi-exponential model characterized by a fast rise (t_{rise}=0.3 ps) assigned to the $S_1 \rightarrow T_1$ ISC and a slow t_{decay} (>500ps) assigned to all the relaxation processes from the T_1 state to the S_0 ground state. Interestingly, an additional relaxation pathway is observed for the triplet state in the presence of **1b**, with a time constant of about 50 ps, which is associated with the formation of triplet exciplex species as depicted in Fig. 4h. Indeed, the formation of the triplet state is known to lead to a planarization of the benzil molecule,[36] which favours the exciplex formation, as confirmed by our TD-DFT calculations (see Supplementary Section K). We can exclude the 50 ps time constant corresponding to the direct formation of a **7**-**1b** CT state. This is because TAS experiments performed on the **7**-**1b** mixture confirmed that this species gives rise to a characteristic ESA signal at significantly longer wavelengths (around 600 nm) and has much longer dynamics.

Adding to previous experimental evidence and supported by DFT calculations, the findings support the existence of an exciplex between substrates **1b** and **7** under these experimental conditions, while offering a rare report of the activity of this elusive and fleeting intermediate.

The impact of the electronic and steric factors on the diastereodifferentiation process

Having verified the key activity of the exciplex under the light-driven stereodifferentiation processes, we next investigated how steric and electronic parameters can be used to rationally control the stereodifferentiation events. Specifically, we selected α-ketoesters **9** as a molecular probe to monitor the impact of steric and electronic parameters on the reaction outcome, while keeping a constant visible-light source set at 405 nm (Fig. 5). Interestingly, the steric repulsion between the R group and the substituent at the C-2 of the indole **1b** (OTBS) will favor a carbonyl perpendicular orientation in the exciplex, leading to ***10-exo*** (Fig. 5a, exciplex box). However, the ***10-endo*** selectivity will be preferred when favoring a **π**–**π** interaction between the aryl group of **9** and the aromatic indole core (Fig. 5a, EDA-complex box).

Evaluation of the electronic factors

We began by evaluating the impact of the electronic factors on the reaction outcome (Fig. 5b). First, we selected various α-ketoesters **9** recording the corresponding UV-Vis spectra in the presence of **1b**, thus assessing their ability to generate an EDA complex. In the case of α-ketoester with Ar = 3,5-CF_3Ph, we observed a red-shifted CT band (see Supplementary Section G). Additionally, the highly negative ΔG_{PET} = -17.1 kcal·mol^{-1} measured was consistent with the formation and activity of an EDA complex. No spectral variations were registered for the other α-ketoesters. We next examined the experimental outcome for all the substates under a 405 nm irradiation (Fig. 5b).

Using a visible-light source was crucial because it enabled the activity of the exciplex and the EDA complex pathways (see Supplementary Section G). This meant that the electronic and steric parameters were the key features in governing the selectivity of these photoreactions. In fact, both the EDA complex and free α-ketoesters absorb light under

these conditions. Only the PB reaction with the electron-deficient 3,5-CF_3Ph α-ketoester was highly *endo*-selective (84:16 d.r., Fig. 5b). The other α-ketoesters showed no ground-state association with **1b**, while maintaining a high level of exergonicity (ΔG_{PET} in the range of -6.0 to -9.5 kcal·mol^{-1}, Fig. 5b) and resulting in similar d.r. of about 70:30.[11, 24]

We depicted the differences in reactivity by plotting the obtained experimental d.r. against the E_{red} of **9** and highlighting the different behavior of the 3,5-CF_3Ph α-ketoester (Fig. 5b, right).

Evaluation of the steric factors

We then investigated the role of the steric factors, tuning the R group within **9** (Fig. 5c). The Charton analysis allowed us to compare the sensitivities (ψ) of the two different manifolds (EDA complex versus exciplex)[41–43]. When increasing the R size (from Me to ^{i}Pr), the *endo:exo* selectivity was reversed, passing from 74:26 to 43:57 d.r. for Ar = Ph (exciplex manifold), and from 84:16 to 45:55 d.r. for Ar = 3,5-CF_3Ph (EDA complex manifold). We rationalize this trend as reflecting an increased steric repulsion between the R group and the OTBS, favoring the perpendicular approach. Nevertheless, the EDA complex manifold experiences a 1.5 increased sensitivity (ψ = -1.51 versus ψ = -2.23 for the exciplex and EDA manifolds, respectively), in agreement with a greater dependence of the parallel approach (π–π interactions) towards steric variations. Finally, we sought to use these findings to deliberately alter the diastereoselective outcome of the PB process by manipulating the steric factors. It is worth mentioning that a light-diastereodifferentiation process was also observed for the reaction between the α-ketoester **9** (Ar = 3,5-CF_3Ph) and the indole **1b**, with the d.r. *endo:exo* passing from 84:16 under 370 nm irradiation to 57:43 under a 427 nm irradiation at -78°C. The lower d.r. variation registered with respect to the reaction performed with benzil **8** is likely because of the very similar absorption profile between the EDA complex and the single substrate (See Supplementary Section G). We selected the 3,5-CF_3Ph α-ketoester because it is the only substrate that formed an EDA complex with **1b** (ψ = -2.23). We observed an initial d.r. of 84:16 in favor of the *endo* product. The *endo* selectivity increased slightly at 40 °C (89:11). Extensive studies performed by Inoue, Mori and Abe have demonstrated that the use of high temperature (>40 °C) generally favours more strongly interacting such as π–π stacked EDA complexes over more flexible structures such as an exciplex[31]. When passing from R = Me to R = ^{i}Pr, the *endo:exo* selectivity was reversed with a d.r. of 45:55 and further magnified to 16:84 when lowering the temperature (Fig. 6). We thus isolated and characterized the elusive *exo*-isomer of oxetane **10** in synthetically useful isolated yield (58%). These results demonstrate that simple structural variations (Me versus ^{i}Pr) in the starting material can dramatically alter the stereochemical outcome of light-driven processes. The importance of the proper light-source selection is also key. No variations were observed when running the reaction at 370 nm. Moreover, these results indicate that overlooked minor modifications of a substrate can have a tremendous impact on the reaction outcome of [2+2] photocycloadditions.

Following the rational approach used for the previous reaction partners, computational analysis was performed (see Supplementary Section K). We computed the EDA complexes and the corresponding vertical excitations between the α-ketoester (**9**, R = Me) and indole

1b. Remarkably, the corresponding excited state (S_1, HOMO-LUMO contribution=94.4%) of the EDA complex in the *endo* configuration (major diastereoisomer) has a larger charge-transfer character (μ=15.8 D) than the *exo* geometry (μ=14.3 D). This trend is in agreement with previous data on the benzil-indole couple. Moreover, similarly to the **1b**-**2b** exciplex, the complex in the triplet state between **1b** and **9** (R = Me) possesses a large dipole moment (m=15.9 D), as reflected by the charge transferred (0.95) from indole to the ketone, which supports the PET-based pathway.

Generality and synthetic potential of the developed diastereodifferentiation processes

Having established two alternative yet complementary methods to govern the stereochemical outcome of the PB reaction, we sought to extend our findings to different carbonyl precursors and to other types of indole derivatives (Fig. 7a). We selected different indoles characterized by various steric and electronic modifications at C-5 and C-6. These new substrates were then subject to the light-driven and the steric factor diastereodifferentiation process under the developed conditions. When changing the light source from UV (370 nm) to visible light (456 nm), a significant variation in the d.r. was observed in all cases. In particular, the presence of an electron donating group, EDG (OMe) stabilized the EDA complex, resulting in higher *exo*-selectivity (53:47). However, the presence of an electron withdrawing group EWG (CF3) did not particularly alter the reaction outcome, demonstrating the robustness of our findings.

In terms of the steric parameters, switching from Me-to ^{i}Pr-α-ketoester dramatically changed the stereochemical outcomes, with the d.r. inverted in all cases. Specifically, the electron-rich OMe group induces an EDA-complex manifold prevalence, while the CF3 group favors the exciplex manifold by disfavoring the **π**–**π** interactions with the electron-deficient α-ketoester **9**.

After evaluating alternative indole derivatives, we explored the preparative potential of the developed light diastereodifferentiation process. The reaction between benzil **7** and indole **1b** was readily implemented into a flow reactor (Fig. 7b and Supplementary Section I)[44]. The reaction in flow furnished identical results with a shorter residence time (40 min)[45]. Furthermore, under the flow conditions, we ran the reaction at 1 mmol scale, isolating both the **8-endo** and the **8-exo** product with an overall yield as high as 88% and 0.57 g. This unprecedented light stereodifferentiation flow process lays the foundation for the use of our protocol in semipreparative medicinal chemistry settings[46, 47].

Conclusion

In conclusion, we have been able to gain control over the stereochemical outcome of light-driven [2+2] heterocycloaddition reactions involving diverse types of carbonyls and indole derivatives. Our results are based on experimental results and corroborated by in-depth investigations of the reaction mechanisms performed by photodynamic analyses, TAS-experiments and supported by spectroelectrochemistry and DFT calculations. With a rational approach, we have revealed the major role of a visible-light-driven EDA complex manifold that can channel the reactivity towards unconventional diastereoselectivity. The often-overlooked effect of the light-source variation was exploited for the development of

new light-stereodifferentiation reactions (d.r. *endo:exo* passing from >99:<1 up to 43:57). Additionally, the punctual modulation of the steric parameters of the starting ketone allows access to unprecedented diastereoinversion events under visible-light irradiation (d.r. *endo:exo* passing from 89:11 to 16:84). The generality and synthetic utility of our findings was further proved for a series of structurally diverse indoles (Fig. 7) and by implementing the light stereodifferentiation process in flow (Fig. 7c).

Our study demonstrates how the mechanistic understanding of light-driven processes can increase their synthetic potential to previously inaccessible structural targets. Further, we envisage a widespread utilization of our approach to the development of novel and selective photoreactions as well as to the mechanistic elucidation of unconventional light-driven reactivity.

Methods

General setup of the light-driven [2+2] cycloaddition reaction

The indole (1 equiv.) and the ketone (1 equiv.) substrates were added into a glass 4 mL glass vial. The solvent was added, and the solution was rapidly degassed with Ar for 1 min. The vial was placed at 5 cm distance from the light source. The reaction was stirred vigorously. To maintain a stable reaction temperature one fan was placed at the top of the photoreactor (20±2 °C) and the temperature was controlled by a thermometer (see Supplementary Fig. S.A.4). The crude reaction mixture was analysed by ^{1}H-NMR spectroscopy to determine the product distribution. The isolated yield was afforded after column chromatography on silica gel.

Supplementary Material

Refer to Web version on PubMed Central for supplementary material.

Acknowledgements

L.D. thanks MUR (Ministero dell'Università) for funding PRIN 2020927WY3_002 and the European Union, European Research Concilium (ERC) Starting Grant SYNPHOCAT (n° 101040025). L.D. thanks the Cariparo, project Synergy within the call Ricerca Scientifica d'Eccellenza 2018 for funding. P.C. thanks the University of Padova, Seal of Excellence@UNIPD, QuantaCOF for funding. Pietro Franceschi (Department of Chemical Sciences, University of Padova, Via Marzolo 1, 35131 Padova, Italy), Philip Andreetta (Department of Chemical Sciences, University of Padova, Via Marzolo 1, 35131 Padova, Italy), and Gianluca Simionato (Department of Chemical Sciences, University of Padova, Via Marzolo 1, 35131 Padova, Italy) are acknowledged for preliminary experiments. Dr Sara Bonacchi (Department of Chemical Sciences, University of Padova, Via Marzolo 1, 35131 Padova, Italy) is acknowledged for insightful discussions.

Data availability statement

All relevant data supporting the findings of this study, including experimental procedures and compound characterization, NMR spectra and other spectroscopic analysis are available within the article and its Supplementary Information.

References

1. Yoon TP, Ischay MA, Du J. Visible light photocatalysis as a greener approach to photochemical synthesis. Nat Chem. 2010; 2: 527–532. [PubMed: 20571569]
2. Minisci F, et al. Additions and Corrections Polar Effects in Free-Radical Reactions Selectivity and Reversibility in the Homolytic Benzylation of Protonated Heteroaromatic Bases (Journal of Organic Chemistry (1986) 51(22) (4326)). Journal of Organic Chemistry. 1986; 51: 4326.
3. Shaw MH, Twilton J, MacMillan DWC. Photoredox Catalysis in Organic Chemistry. Journal of Organic Chemistry. 2016; 81: 6898–6926. [PubMed: 27477076]
4. Mateos J, et al. A visible-light Paternò-Büchi dearomatisation process towards the construction of oxeto-indolinic polycycles. Chem Sci. 2020; 11: 6532–6538. [PubMed: 34094119]
5. Franceschi P, Mateos J, Vega-Peñaloza A, Dell'Amico L. Microfluidic Visible-Light Paternò–Büchi Reaction of Oxindole Enol Ethers. Eur J Org Chem. 2020; 43: 6718–6722.
6. Zheng J, Dong X, Yoon TP. Divergent Photocatalytic Reactions of α-Ketoesters under Triplet Sensitization and Photoredox Conditions. Org Lett. 2020; 22: 6520–6525. [PubMed: 32806138]
7. Paternò E, Chieffi G. Sintesi in Chimica Organica per Mezzo Della Luce. Nota II. Composti Degli Idrocarburi Non Saturi Con Aldeidi e Chetoni. Gazz Chim Ital. 1909; 39: 341.
8. Büchi G, Inman CG, Lipinsky ES. Light-catalyzed Organic Reactions. I. The Reaction of Carbonyl Compounds with 2-Methyl-2-butene in the Presence of Ultraviolet Light. J Am Chem Soc. 1954; 76: 4327–4331.
9. Bull JA, Croft RA, Davis OA, Doran R, Morgan KF. Oxetanes: Recent Advances in Synthesis, Reactivity, and Medicinal Chemistry. Chemical Reviews. 2016; 116: 12150–12233. [PubMed: 27631342]
10. Turro NJ, et al. Molecular photochemistry of alkanones in solution: α-cleavage, hydrogen abstraction, cycloaddition, and sensitization reactions. Acc Chem Res. 1972; 5: 92–101.
11. Mattay J, Gersdorf J, Buchkremer K. Photoreactions of biacetyl with electron-rich olefins. An extended mechanism. Chem Ber. 1987; 120: 307–318.
12. Fréneau M, Hoffmann N. The Paternò-Büchi reaction—Mechanisms and application to organic synthesis. Journal of Photochemistry and Photobiology C: Photochemistry Reviews. 2017; 33: 83–108.
13. Mateos J, Cuadros S, Vega-Peñaloza A, Dell'Amico L. Unlocking the Synthetic Potential of Light-Excited Aryl Ketones: Applications in Direct Photochemistry and Photoredox Catalysis. Synlett. 2022; 33: 116–128.
14. Salem L. Surface Crossings and Surface Touchings in Photochemistry. J Am Chem Soc. 1974; 96: 3486–3501.
15. Griesbeck AG, Abe M, Bondock S. Selectivity control in electron spin inversion processes: Regio- and stereochemistry of Paternò-Büchi photocycloadditions as a powerful tool for mapping intersystem crossing processes. Acc Chem Res. 2004; 37: 919–928. [PubMed: 15609983]
16. Crisenza GEM, Mazzarella D, Melchiorre P. Synthetic Methods Driven by the Photoactivity of Electron Donor-Acceptor Complexes. Journal of the American Chemical Society. 2020; 142: 5461–5476. [PubMed: 32134647]
17. Matsumura K, Mori T, Inoue Y. Wavelength control of diastereodifferentiating Paternó-Büchi reaction of chiral cyanobenzoates with diphenylethene through direct versus charge-transfer excitation. J Am Chem Soc. 2009; 131: 17076–17077. [PubMed: 19891435]
18. Sun D, Hubig SM, Kochi JK. Oxetanes from [2+2] cycloaddition of stilbenes to quinone via photoinduced electron transfer. J Org Chem. 1999; 64: 2250–2258.

19. Zhang Y, Xue J, Gao Y, Fun HK, Xu JH. Photoinduced [2+2] cycloadditions (the Paterno–Büchi reaction) of 1-acetylisatin with enol ethers—regioselectivity, diastereoselectivity and acid catalysed transformations of the spirooxetane products. J Chem Soc Perkin 1. 2002; 2: 345–353.
20. Kandukuri SR, et al. X-ray characterization of an electron donor-acceptor complex that drives the photochemical alkylation of indoles. Angew Chemie - Int Ed. 2015; 54: 1485–1489.
21. Buzzetti L, Crisenza GEM, Melchiorre P. Mechanistic Studies in Photocatalysis. Angewandte Chemie - International Edition. 2019; 58: 3730–3747. [PubMed: 30339746]
22. Freilich SC, Peters KS. Observation of the 1,4-Biradical in the Paterno-Buchi Reaction. J Am Chem Soc. 1981; 103: 6255–6257.
23. Rehm D, Weller A. Kinetics of Fluorescence Quenching by Electron and H-Atom Transfer. Isr J Chem. 1970; 8: 259–271.
24. Mattay J, Runsink J, Rumbach T, Ly C, Gersdorf J. Selectivity and Charge Transfer in Photoreactions of α, α, α-Trifluorotoluene with Olefins. J Am Chem Soc. 1985; 107: 2557–2558.
25. Mattay J, Gersdorf J, Buchkremer K. Photoreactions of Biacetyl with Electron-Rich Olefins. An Extended Mechanism. Chem Ber. 1987; 120: 307–318.
26. Mieres-Perez J, Costa P, Mendez-Vega E, Crespo-Otero R, Sander W. Switching the Spin State of Pentafluorophenylnitrene: Isolation of a Singlet Arylnitrene Complex. J Am Chem Soc. 2018; 140: 17271–17277. [PubMed: 30430835]
27. Gutiérrez-Hernández A, et al. Deep Eutectic Solvent Choline Chloride/ p-toluenesulfonic Acid and Water Favor the Enthalpy-Driven Binding of Arylamines to Maleimide in Aza-Michael Addition. J Org Chem. 2021; 86: 223–234. [PubMed: 33232142]
28. Mori T, Inoue Y. Charge-transfer excitation: Unconventional yet practical means for controlling stereoselectivity in asymmetric photoreactions. Chem Soc Rev. 2013; 42: 8122–8133. [PubMed: 23832068]
29. Trost BM, Dong G, Vance JA. Cyclic 1,2-Diketones as Core Building Blocks: A Strategy for the Total Synthesis of (–)-Terpestacin. Chem – A Eur J. 2010; 16: 6265–6277.
30. Samanta S, Roy D, Khamarui S, Maiti DK. Ni(ii)-salt catalyzed activation of primary amine-sp3Cα-H and cyclization with 1,2-diketone to tetrasubstituted imidazoles. Chem Commun. 2014; 50: 2477–2480.
31. Matsumura K, Mori T, Inoue Y. Solvent and temperature effects on diastereodifferentiating paternó-büchi reaction of chiral alkyl cyanobenzoates with diphenylethene upon direct versus charge-transfer excitation. J Org Chem. 2010; 75: 5461–5469. [PubMed: 20704423]
32. Saito H, Mori T, Wada T, Inoue Y. Diastereoselective [2 + 2] Photocycloaddition of Stilbene to Chiral Fumarate. Direct versus Charge-Transfer Excitation. J Am Chem Soc. 2004; 126: 1900–1906. [PubMed: 14871123]
33. Aoki Y, Matsuki N, Mori T, Ikeda H, Inoue Y. Exciplex ensemble modulated by excitation mode in intramolecular charge-transfer dyad: Effects of temperature, Solvent polarity, and wavelength on photochemistry and photophysics of tethered naphthalene-dicyanoethene system. Org Lett. 2014; 16: 4888–4891. [PubMed: 25207472]
34. Nagasaki K, Inoue Y, Mori T. Entropy-Driven Diastereoselectivity Improvement in the Paternò–Büchi Reaction of 1-Naphthyl Aryl Ethenes with a Chiral Cyanobenzoate through Remote Alkylation. Angew Chemie - Int Ed. 2018; 57: 4880–4885.
35. D'Auria M. The Paternò-Büchi reaction-a comprehensive review. Photochemical and Photobiological Sciences. 2019; 18: 2297–2362. [PubMed: 31273370]
36. Griesbeck AG, Buhr S, Fiege M, Schmickler H, Lex J. Stereoselectivity of Triplet Photocycloadditions:1 Diene-Carbonyl Reactions and Solvent Effects. J Org Chem. 1998; 63: 3847–3854.
37. Harris, CB, Ippen, EP, Mourou, G, Zewail, AH. Ultrafast Phenomena VIII. Springer; Berlin, Heidelberg: 1993.
38. Ikeda N, Koshioka M, Masuhara H, Yoshihara K. Picosecond dynamics of excited singlet states in organic microcrystals: Diffuse reflectance laser photolysis study. Chem Phys Lett. 1988; 150: 452–456.
39. Singh AK, Palit DK, Mittal JP. Conformational relaxation dynamics in the excited electronic states of benzil in solution. Chem Phys Lett. 2002; 360: 443–452.

40. Fang TS, Singer LA. Variable temperature studies on the luminescence from Benzil in a polymethylmethacrylate glass. An example of matrix controlled photorotamerism. Chem Phys Lett. 1978; 60: 117–121.

41. Charton M. Steric effects. I. Esterification and acid-catalyzed hydrolysis of esters. J Am Chem Soc. 1975; 97: 1552–1556.

42. Harper KC, Bess EN, Sigman MS. Multidimensional steric parameters in the analysis of asymmetric catalytic reactions. Nature Chemistry. 2012; 4: 366–374.

43. Sigman MS, Miller JJ. Examination of the Role of Taft-Type Steric Parameters in Asymmetric Catalysis. J Org Chem. 2009; 74: 7633–7643. [PubMed: 19813764]

44. Cambié D, Bottecchia C, Straathof NJW, Hessel V, Noël T. Applications of Continuous-Flow Photochemistry in Organic Synthesis, Material Science, and Water Treatment. Chem Rev. 2016; 116: 10276–10341. [PubMed: 26935706]

45. Mateos J, et al. A microfluidic photoreactor enables 2-methylbenzophenone light-driven reactions with superior performance. Chem Commun. 2018; 54: 6820–6823.

46. Chapman SJ, Swords WB, Le CM, Guzei IA, Toste FD, Yoon TP. Cooperative Stereoinduction in Asymmetric Photocatalysis. J Am Chem Soc. 2022; 144: 4206–4213. [PubMed: 35192768]

47. Poplata S, Tröster A, Zou Y-Q, Bach T. Recent Advances in the Synthesis of Cyclobutanes by Olefin [2 + 2] Photocycloaddition Reactions. Chem Rev. 2016; 116: 9748–9815. [PubMed: 27018601]

Europe PMC Funders Author Manuscripts

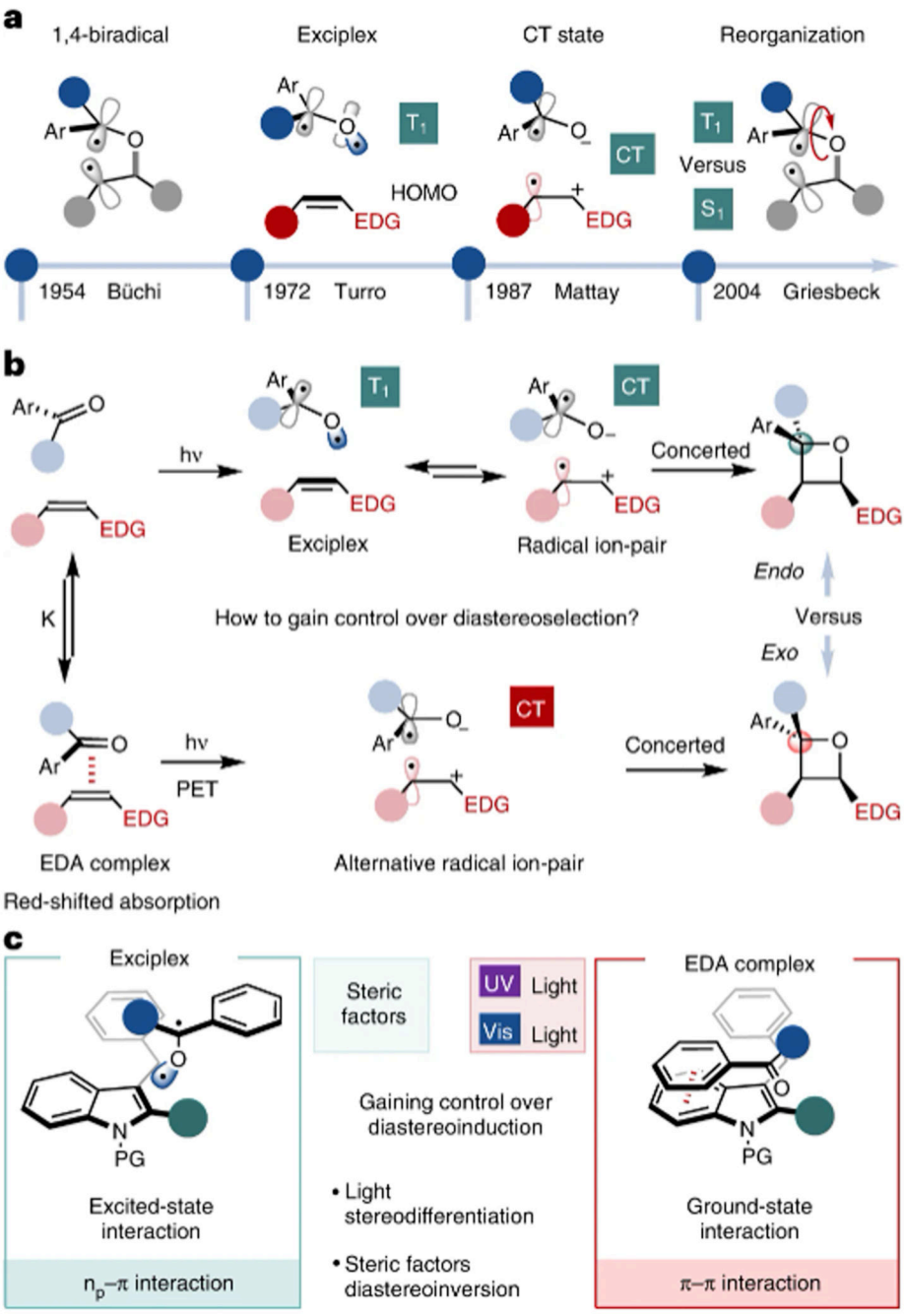

Figure 1. The [2+2] heterocycloaddition process.

a) Mechanisms and predicting models of the Patemò-Büchi reaction and applications. **b)** Working hypothesis of the present work: controlling the nature of the reactive intermediate can lead to diverse stereocontrol. **c)** The current case study: Paternò-Büchi reaction with indoles. CT, charge transfer; T_1, triplet state, S_1, singlet state; EDG, electron donating group; EWG, electron withdrawing group; PET, photoinduced electron transfer; EDA, electron donor acceptor; PG, protecting group.

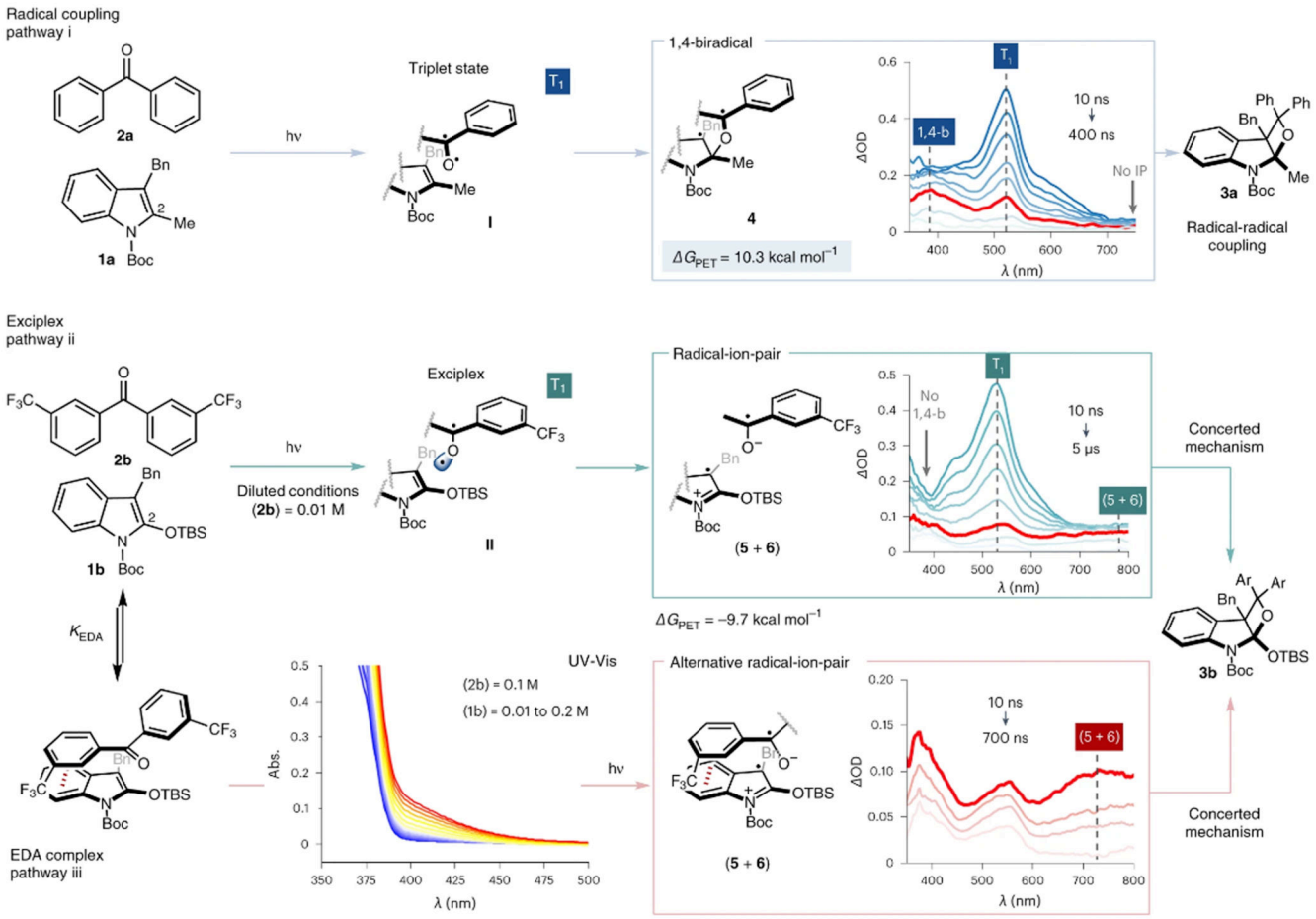

Figure 2. Spectroscopic studies of the Paternò-Büchi reaction and identification of three different possible pathways.

Pathway i relies on radical coupling, pathway ii proceeds through an exciplex intermediate and pathway iii proceeds through an EDA complex intermediate. The group at position 2 of the indole is highlighted because it impacts the donor ability of the molecule. T_1, triplet state; 1,4-b, 1,4-biradical; Bn, benzyl; TBS, *tert-Butyl* dimethyl silyl; OD, optical density.

Europe PMC Funders Author Manuscripts

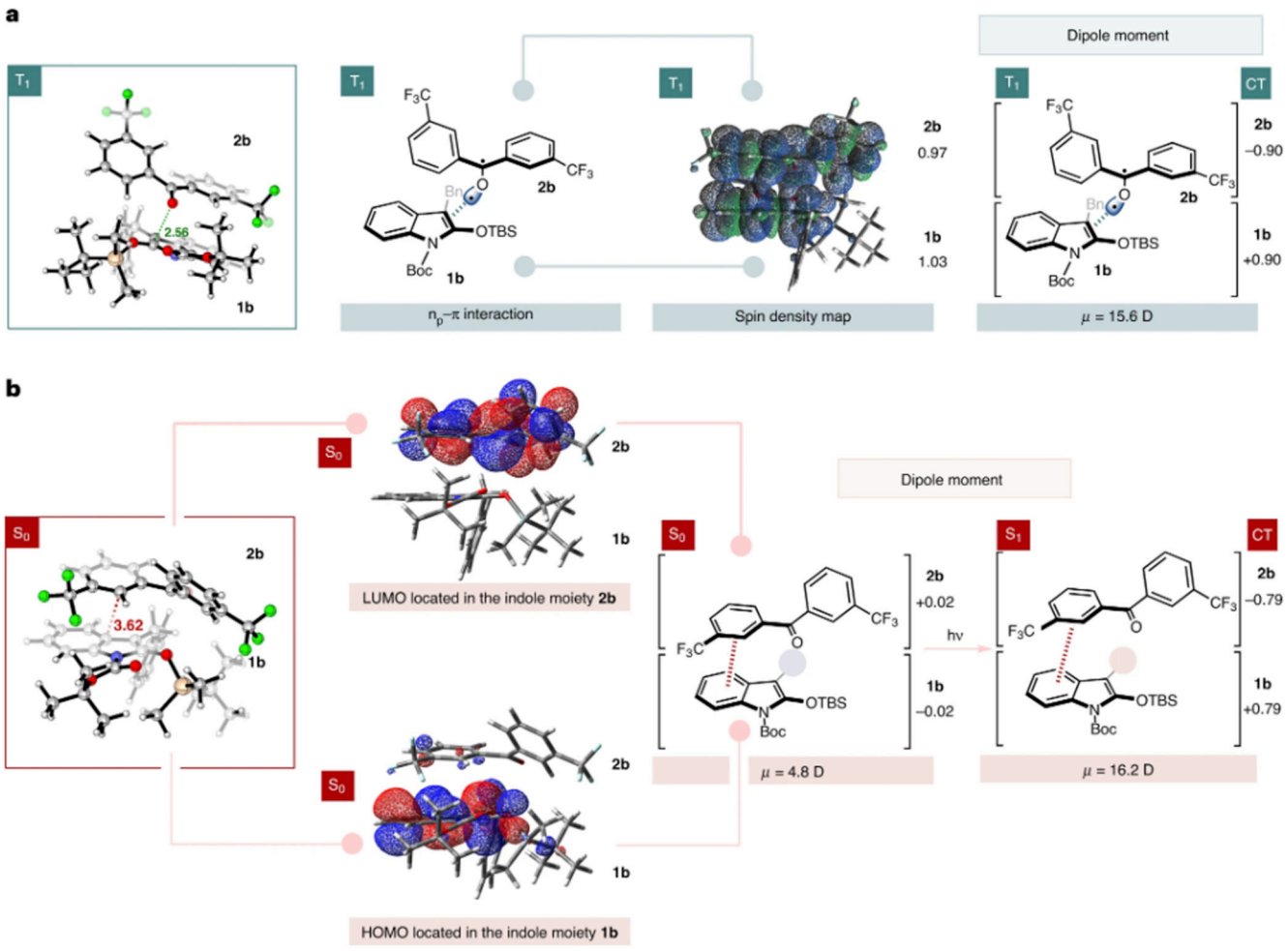

Figure 3. Computational insights into the exciplex and EDA-complex manifolds.

a) The excited-state (T_1) exciplex arrangement related to reaction pathway ii. **b)** The ground-state (S_0) EDA-complex arrangement related to pathway iii. Calculations performed using the U)M06-2X/6-311++G(d,p)/_IEFPCM(acetone) level of theory. CT, charge transfer; T_1, triplet state; S_0, ground state; LUMO, lowest unoccupied molecular orbital; HOMO, highest occupied molecular orbital.

Europe PMC Funders Author Manuscripts

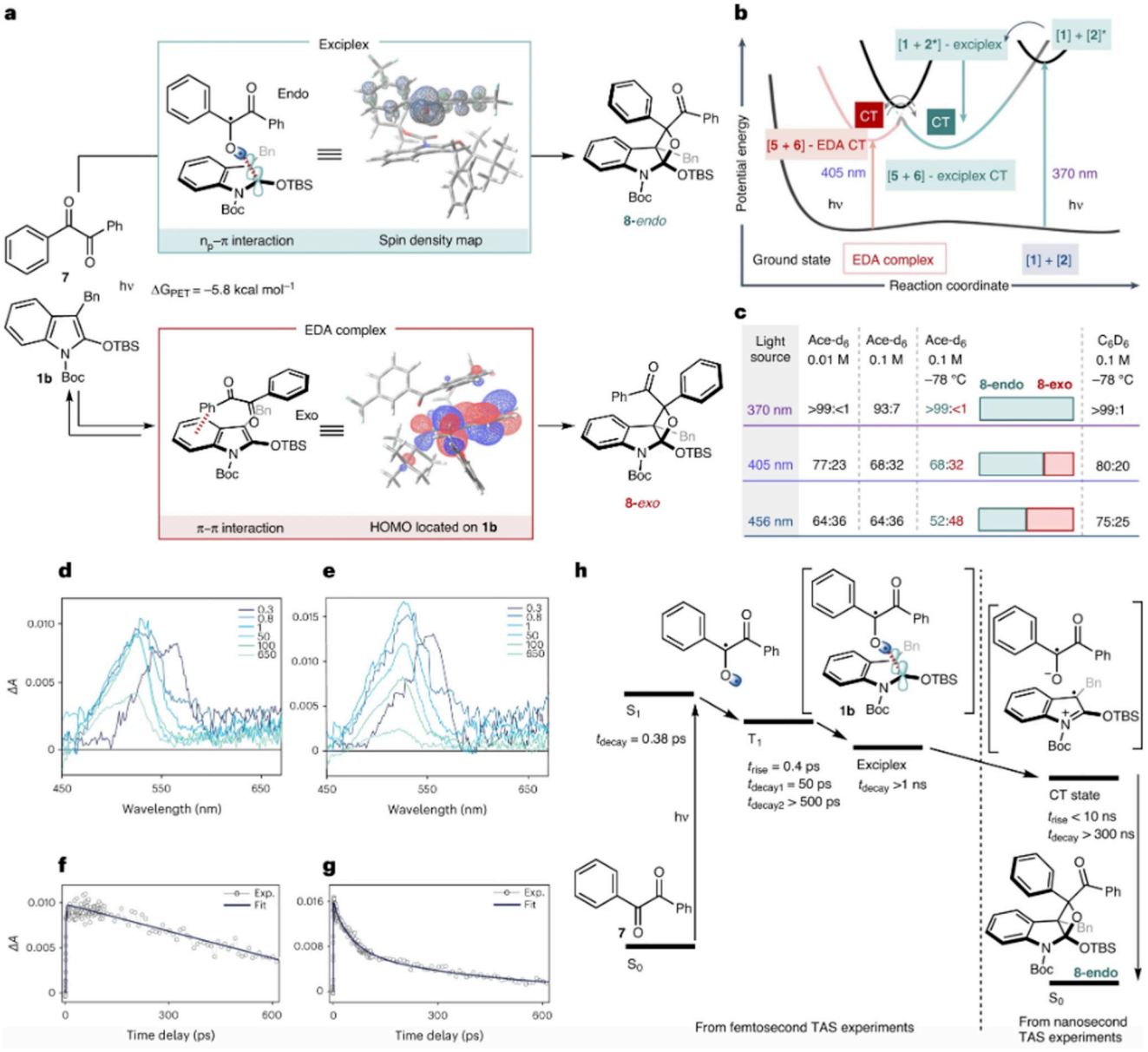

Figure 4. Diastereodivergent pathways with benzil.

a) Paternò-Büchi reaction between indole **1b** and 1,2-diketone **7**. **b)** Simplified potential energy surface diagram of the PB reaction. **c)** Observed experimental results. The reported d.r. values refer to *endo:exo* d.r. The d.r. values are inferred by U-NMR spectroscopic analysis on the crude reaction mixture. **d)** and **e)** Transient absorption spectra (ΔA versus probe wavelength) for **7** and the mixture 1:1 of **7** and **1b** at selected delay times, respectively. 0.03 M, acetone, T=298 K. Excitation at 400 nm. **f)** and **g)** Decay traces (ΔA versus time delay) extracted at a probe wavelength of 525 nm. The dots represent experimental points, while blue lines indicate the result of the fitting procedure. **h)** Energy level diagram and photophysical behaviour of molecular components **7** and **1b** upon 400 nm photoexcitation (pathway ii). CT, charge transfer; T_1, triplet state; S_0, ground state; HOMO,

highest occupied molecular orbital; Ace, acetone; TAS, transient absorption spectroscopy; t, time, A; absorbance.

Europe PMC Funders Author Manuscripts

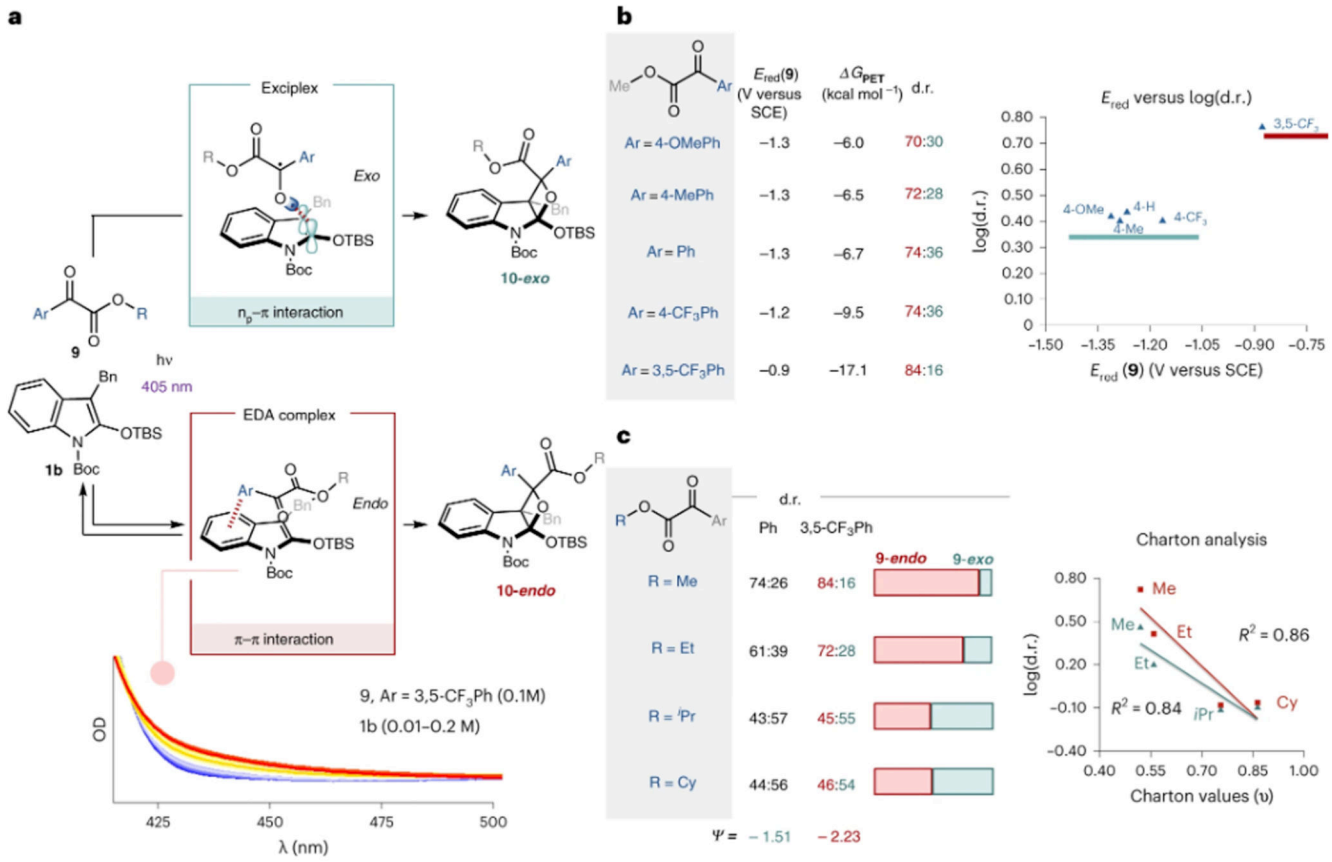

Figure 5. Diastereodivergent pathways with α-ketoesters.

a) Paternò-Büchi reaction between indole **1b** and ketoesters **9** and proposed reaction manifolds. **b)** Evaluation of the electronic factors to control diastereoselectivity. **c)** Evaluation of the steric factors to control diastereoselectivity. The reported d.r. values refer to *endo:exo* d.r. The d.r. values are inferred by ^{1}H-NMR spectroscopic analysis on the crude reaction mixture. Ψ, sensitivity; SCE, silver calomel electrode; Cy, cyclohexyl.

Europe PMC Funders Author Manuscripts

Europe PMC Funders Author Manuscripts

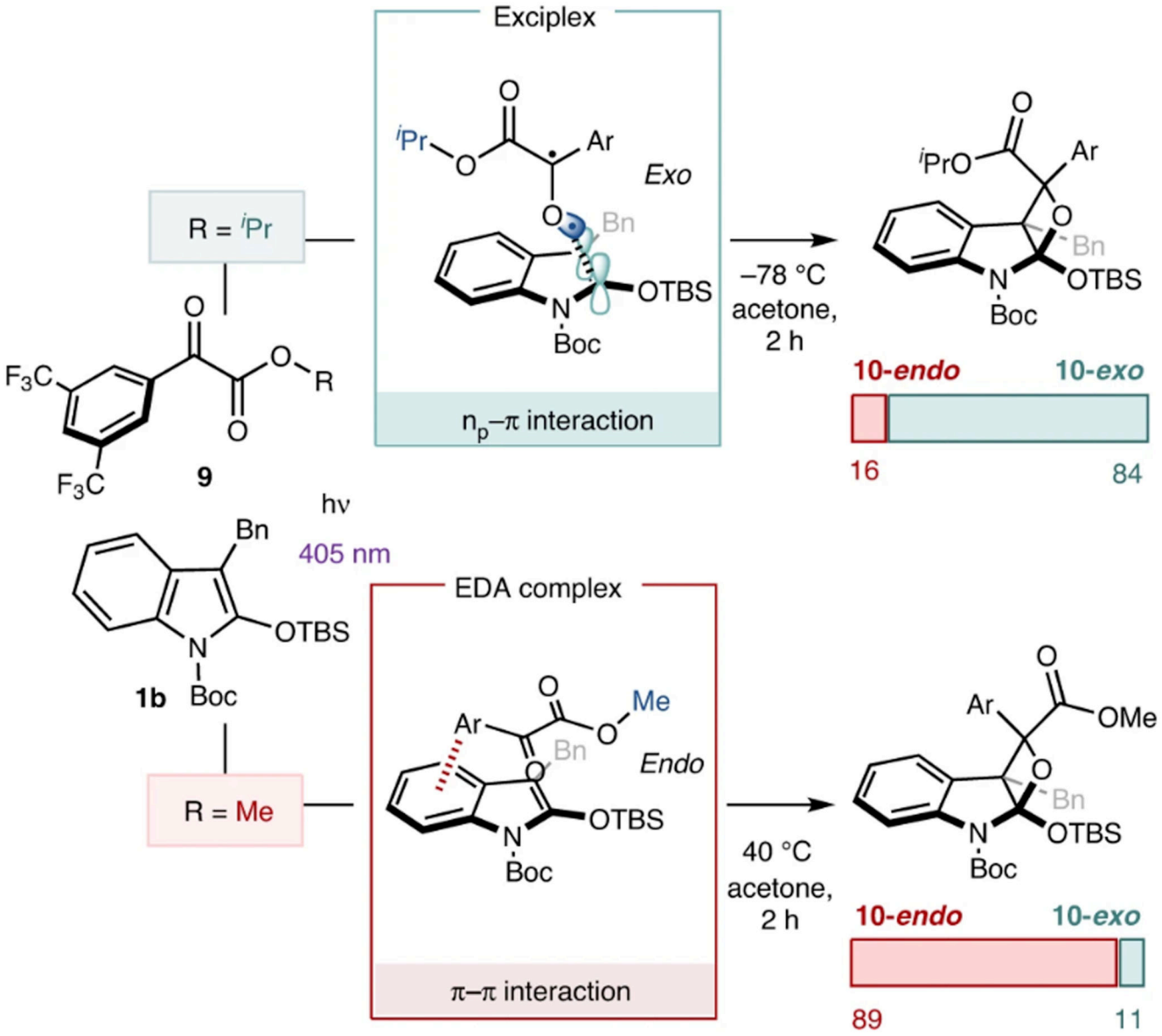

Figure 6. Using steric parameters to gain control over diastereoselection.

The d.r. is controlled by changing the size of the R group. Ar, 1,3-CF_3Ph; Boc, *tert*-butyloxycarbonyl; TBS, *tert*-Butyl dimethyl silyl.

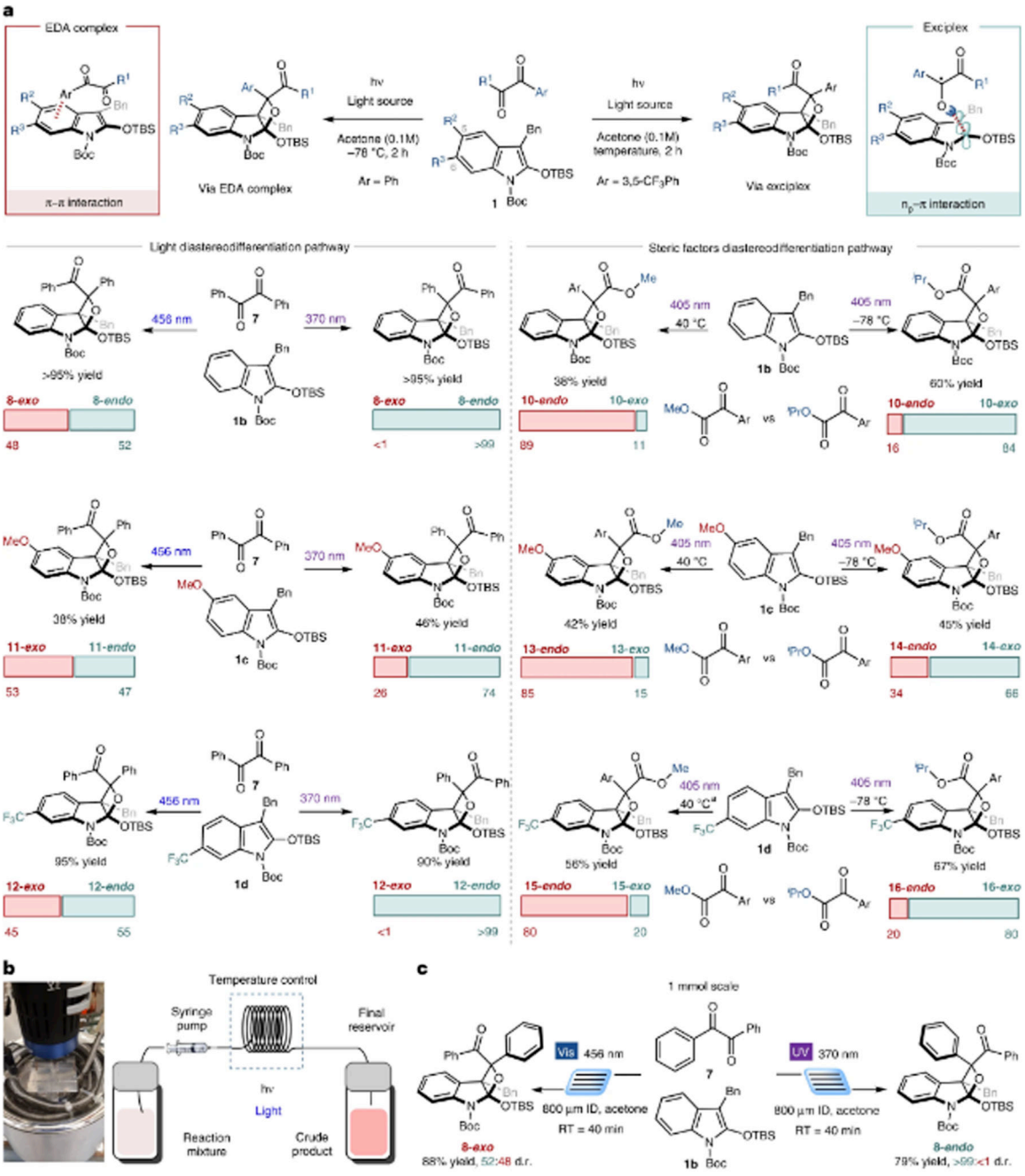

Figure 7. Generality of the developed light-driven process and in-flow implementation.

a) Generality of the developed light-driven and steric factors for controlling diastereodifferentiation processes. [a]The reaction was performed in PhMe and the same reaction in acetone gave inferior *endo:exo* selectivity with a d.r. of 40:60. All the yields refer to a reaction time of 2 h and no attempts were made to optimize the yield values. The reported d.r. values refer to *endo:exo* d.r., and are inferred by ^{1}H-NMR spectroscopic analysis on the crude reaction mixture. **b)** Photo and schematic representation of the

Europe PMC Funders Author Manuscripts

microfluidic setup used in this study. **c)** 1 mmol scale reaction performed under microflow. ID, internal diameter; RT, room temperature.

Europe PMC Funders Author Manuscripts